

## Control of wave packet spreading in nonlinear finite disordered lattices

Rodrigo A. Vicencio<sup>1</sup> and Sergej Flach<sup>1</sup>

<sup>1</sup>*Departamento de Física, Facultad de Ciencias, Universidad de Chile, Santiago, Chile*

<sup>2</sup>*Max-Planck-Institut für Physik komplexer Systeme, Nöthnitzer Strasse 38, D-01187 Dresden, Germany*

(Received 11 September 2008; published 27 January 2009)

In the absence of nonlinearity all normal modes (NMs) of a chain with disorder are spatially localized (Anderson localization). We study the action of nonlinearity, whose strength is ramped linearly in time. It leads to a spreading of a wave packet due to interaction with and population of distant NMs. Eventually nonlinearity-induced frequency shifts take over and the wave packet becomes self-trapped. On finite chains a critical ramping speed is obtained, which separates delocalized final states from localized ones. The critical value depends on the strength of disorder and is largest when the localization length matches the system size.

DOI: [10.1103/PhysRevE.79.016217](https://doi.org/10.1103/PhysRevE.79.016217)

PACS number(s): 05.45.-a, 03.75.Lm, 42.65.Wi, 63.20.Pw

### I. INTRODUCTION

Spatial discreteness and nonlinearity have been probed recently within the context of Bose-Einstein condensates (BECs) in optical lattices [1] and propagation of light in nonlinear optical waveguide arrays [2], to name a few. The balance between these ingredients allows for the excitation of localized structures known as *discrete breathers* or *solitons* [3]. Localization is due to nonlinearity induced frequency shifts, which tune a localized excitation out of resonance with the surrounding nonexcited extended lattice modes and is also known as *self-trapping*.

The normal modes (NMs) of a one-dimensional *linear* chain with uncorrelated random potential are spatially localized (Anderson localization). Therefore any wave packet that which is initially localized remains localized for all time [4]. Anderson localization is harvesting on destructive interference and phase coherence, despite the fact that the frequency of a localized NM is not tuned out of resonance with other NMs. From the experimental point of view, disorder can be easily implemented in BECs by tuning the wavelength of laser beams [5] or by superimposing a speckle pattern [6]. Recently experiments have been reported that observe Anderson localization for noninteracting BECs [7]. In optics, disorder can be implemented in waveguide arrays by altering the fabrication process [8,9] or, in optically induced lattices, by adding a speckle beam [10].

Nonlinearity induces an interaction between NMs and frequency shifts. While an interaction favors delocalization [11–13], frequency shifts may lead to self-trapping and again to localization [14]. Continuation of NMs into the nonlinear regime may keep localization, but also delocalize excitations via resonances [15]. Experimental studies of the combined action of nonlinearity and disorder are possible both in BEC systems and in optics [8–10,16].

According to Ref. [13], any initial wave packet in a disordered potential and a fixed value of the nonlinearity parameter define three regimes: weak, intermediate, and strong nonlinearity. The weak nonlinearity regime is characterized by Anderson localization on potentially large time scales and subsequent detraping and spreading. The intermediate regime is yielding spreading from scratch. The spreading continues despite the fact that the nonlinear frequency shifts

weaken, since that is balanced by the increase in the number of excited NMs. Finally the strong nonlinearity regime leads to partial self-trapping; i.e., a part of the wave packet self-traps and does not delocalize, while the remaining part spreads again. The spreading is universal and subdiffusive, therefore rather slow, posing challenges for experimental studies, where one has to compete with dissipation mechanisms that lead to dephasing.

Here we study how to control the spreading of a wave packet in a finite lattice by ramping the strength of nonlinearity in time. The increase of nonlinearity with time counteracts the above diminishing of nonlinear frequency shifts and substantially speeds up the spreading process. At the same time, resonant adiabatic excitation of distant NMs can contribute to a spreading as well. A too strong increase of the nonlinearity will finally lead to self-trapping, and the spreading process stops when the wave packet reaches a certain average size which depends on the control parameters. That makes our results also easier accessible for experiments.

### II. MODEL

#### A. Equations of motion

We consider a discrete nonlinear Schrödinger (DNLS) model which describes the propagation of light in nonlinear waveguide arrays or the evolution of a BEC in a periodic optical potential [1,2]. The Hamiltonian

$$\mathcal{H} = \sum_l \left[ \epsilon_l |\psi_l|^2 + (\psi_{l+1} \psi_l^* + \psi_{l+1}^* \psi_l) + \frac{\beta}{2} |\psi_l|^4 \right].$$

The equations of motion are generated with  $-i\partial\psi_l/\partial z = \partial\mathcal{H}/\partial\psi_l^*$ :

$$-i \frac{\partial\psi_l}{\partial z} = \epsilon_l \psi_l + (\psi_{l+1} + \psi_{l-1}) + \beta(z) |\psi_l|^2 \psi_l, \quad (1)$$

where  $\psi_l(z)$  is a complex wave amplitude at site  $l$ . Here  $z$  corresponds to the dynamical variable (propagation coordinate for photons or time for atoms). The nonlinear coefficient  $\beta \equiv \beta(z) \equiv c_0 z^\mu$  increases with  $z$  ( $\mu > 0$ ). We will numerically investigate linear ramping  $\mu=1$  with velocity  $c_0 > 0$ . This can be implemented for the case of a BEC, where the inter-

action between condensed atoms can be described by a single parameter, the scattering length, which can be tuned by an external applied magnetic field. This parameter can be adjusted via Feshbach resonances, and therefore the nonlinear interaction between particles can be tuned and controlled in time [17]. In optical systems, the nonlinearity can be adjusted in the propagation direction ( $z$ ) in the fabrication process of laser-written waveguide arrays [18] or by controlling the doping concentration in photovoltaic samples [19].

The random on-site energies  $\epsilon_l$  are chosen uniformly from the interval  $[-\frac{W}{2}, \frac{W}{2}]$ , where  $W$  is the strength of disorder. The norm  $\mathcal{N} \equiv \sum_l |\psi_l|^2$  is dynamically conserved; i.e., its value does not change with  $z$ . In our calculations,  $\mathcal{N}=1$ . We note that varying the norm is strictly equivalent to varying  $\beta$ . For  $c_0=0$ , Eq. (1) is reduced to the linear eigenvalue problem  $-\lambda_\nu A_{\nu,l} = \epsilon_l A_{\nu,l} + (A_{\nu,l+1} + A_{\nu,l-1})$ . The eigenvectors  $A_{\nu,l}$  are the NMs and the eigenvalues  $\lambda_\nu$  their frequencies.

We analyze normalized distributions  $n_l = |\psi_l|^2 \geq 0$  using the participation number  $P = 1/\sum_l n_l^2$ , which measures the number of the strongest excited sites, and the second moment  $m_2 = \sum_l (l - \bar{l})^2 n_l$ , which measures the size of the wave packet. Here  $\bar{l} = \sum_l l n_l$ .

### B. Linear case $c_0=0$

Let us first consider an infinite system. For  $W=c_0=0$ , solutions of Eq. (1) are extended plane waves  $u_l(z) = u_0 \exp[i(kl - \lambda_k z)]$  with the dispersion relation  $\lambda_k \equiv -2 \cos k$ . The frequencies  $\lambda_k$  are confined to the interval  $[-2, 2]$  ( $k$  is related to the input angle for optics or to the quasimomentum for BEC). The group velocities of the plane waves  $|v_g| \leq 2$ .

For  $W \neq 0$ ,  $c_0=0$ , the frequency spectrum is confined to  $[-2 - \frac{W}{2}, 2 + \frac{W}{2}]$ . The width of the spectrum  $\{\lambda_\nu\}$  is  $\Delta = 4 + W$ . All eigenvectors will be localized in space [4]. The asymptotic spatial decay of an eigenvector is given by  $A_{\nu,l} \sim e^{-\xi l}$ , where  $\xi(\lambda_\nu) \leq \xi(0) \approx 100/W^2$  is the localization length [20]. The NM participation number  $p_\nu = 1/\sum_l A_{\nu,l}^4$  characterizes the spatial extent—localization volume—of the NM. It is distributed around the mean value  $\bar{p} \approx 3.6\xi$  with variance  $\approx (1.3\xi)^2$  [21]. The average spacing of eigenvalues of NMs within the range of a localization volume is therefore  $\Delta\lambda \approx \Delta/\bar{p}$ .

The linear case is characterized by two frequency scales: the width of the spectrum  $\Delta$ , and the average spacing  $\Delta\lambda < \Delta$ . In addition, since we will operate with finite systems, we also have two spatial scales: the localization length  $\xi$  and the system size  $N$ .

We launch a single-site excitation in the center of our system with  $N=100$  and follow its evolution until  $z=z_{max}$  ( $z_{max} \equiv N/4$ ). For  $W=0$ , the fastest plane waves will reach the boundaries exactly at  $z=z_{max}$ . A plot of the corresponding norm profile is shown in Fig. 1(a). The corresponding participation number is  $P \approx 44 = 0.44N$ . Indeed, an almost completely spread wave packet is characterized by roughly  $P = N/2$ , since a strictly homogeneous distribution is counterbalanced by dynamical fluctuations, and therefore, on average, every second site is not excited.

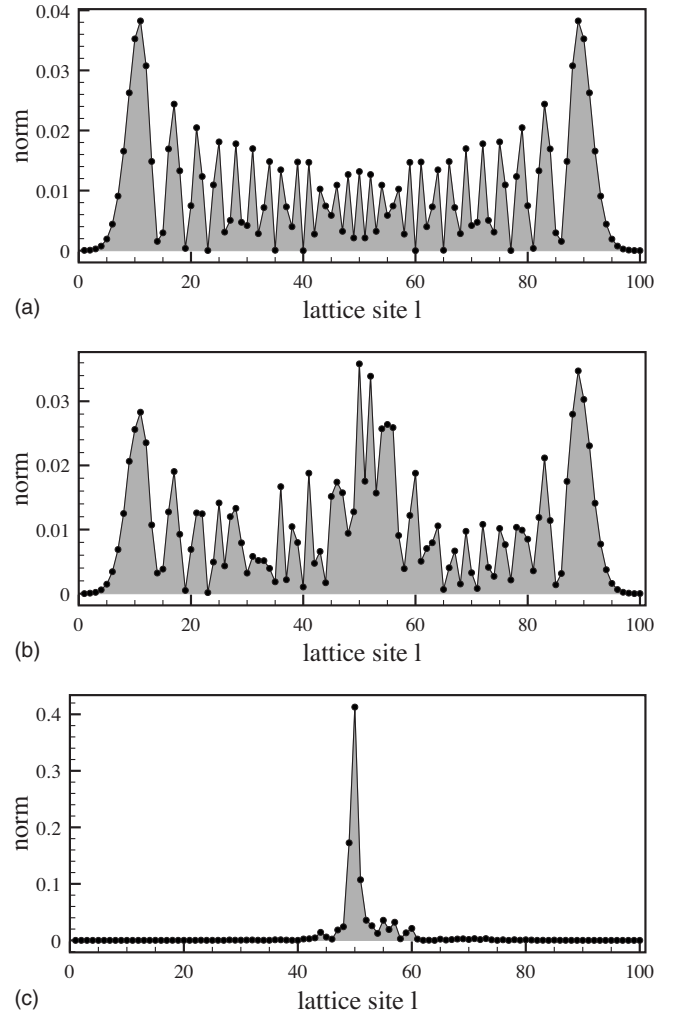


FIG. 1. Linear propagation. Spatial profile at  $z=z_{max}$  for (a)  $W=0$ , (b)  $W=0.5$ , and (c)  $W=3$ .  $N=100$ .

Now we increase the strength of disorder  $W$ . For  $W=1$  the localization length equals the system size. Therefore, for  $W=0.5$  [Fig. 1(b)] we still observe almost full spreading, although the fronts propagate slower. For  $W=3$  [Fig. 1(c)] we observe Anderson localization—the wave packet is confined to the localization volume which is of the order of 20 sites.

We performed runs for 100 realizations and compute the average of the second moment  $m_2$  and of the participation number  $P$  at  $z_{max}$  (see Fig. 2). The second moment  $m_2$  decreases with increasing disorder as expected, showing that waves propagate slower even within the localization volume ( $W < 1$ ) due to disorder-induced backscattering. However, the participation number  $P$  shows a slight increase for weak disorder, with a subsequent (expected) decrease for stronger disorder. For the ordered case  $W=0$ , the chosen initial condition excites one-half of all available NMs. That follows from the reflection invariance of the lattice around the center, where the initial wave packet is placed. All NMs separate into two irreducible groups of even and odd ones, or symmetric and antisymmetric ones, with respect to reflections around the chain center. A single-site excitation in the center excites only even NMs. For weak disorder all NMs start to become excited. Therefore the part of the volume which is

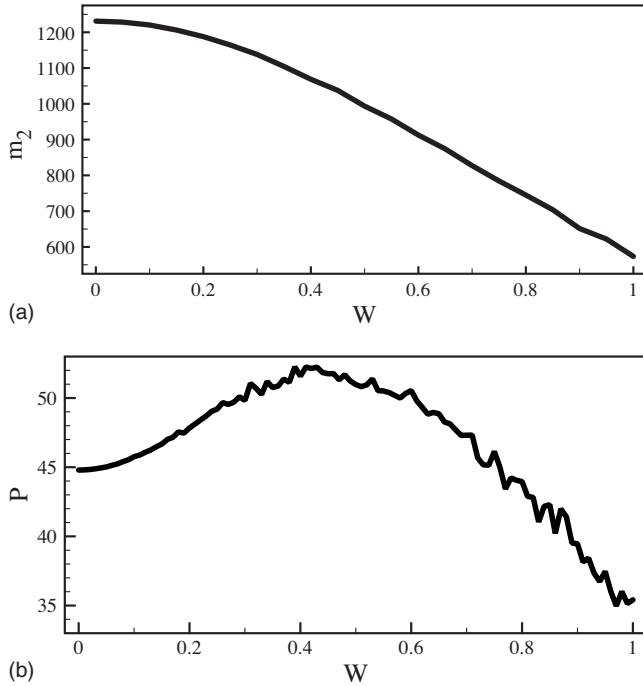


FIG. 2. Linear propagation. (a) Average second moment  $m_2$  measured at time  $z_{max}$  as a function of  $W$ . (b) Same as (a), but for the participation number  $P$ .  $N=100$ , and averaging was performed with 100 realizations.

occupied by the wave packet at some later time is filled more homogeneously. Note that the effect is weak—the participation number increases by  $\sim 15\%$ . That may be due to the fact that at the same time the wave packet spreads less effectively, as follows from the results on the second moment.

### C. Nonlinear case

The equations of motion in normal-mode space read [13]

$$-i\dot{\phi}_\nu = \lambda_\nu \phi_\nu + \beta \sum_{\nu_1, \nu_2, \nu_3} I_{\nu, \nu_1, \nu_2, \nu_3} \phi_{\nu_1} \phi_{\nu_2}^* \phi_{\nu_3}, \quad (2)$$

with the overlap integral

$$I_{\nu, \nu_1, \nu_2, \nu_3} = \sum_l A_{\nu, l} A_{\nu_1, l} A_{\nu_2, l}^* A_{\nu_3, l}. \quad (3)$$

The variables  $\phi_\nu$  determine the complex time-dependent amplitudes of the NMs.

Nonlinearity therefore induces interaction between NMs. In particular, the nonlinearity renormalizes frequencies. If frequencies are shifted out of the spectrum of the linear equation, self-trapping occurs and excitations stay localized for long, maybe infinite, times. We are not aware of a straightforward and unique way to calculate such a frequency shift for a given distribution  $n_l$ . Therefore we will look for suitable estimates. One possibility is to neglect the coupling along the lattice and treat lattice sites as independent. Then the nonlinear frequency shift at site  $l$  is  $\delta\lambda \approx -\beta n_l$ . Another possibility is to derive an effective frequency  $\lambda_{eff}$  for a given state. We treat a state as a stationary one,  $\psi_l(z) = A_l \exp(-i\lambda_{eff}z)$ . We insert this ansatz in (1), multiply this

equation by  $\psi_l^*$ , and sum over all lattice sites:

$$\lambda_{eff} = - \sum_l [\epsilon_l |\psi_l|^2 + \psi_{l+1} \psi_l^* + \psi_{l+1}^* \psi_l + \beta |\psi_l|^4]. \quad (4)$$

At any time  $z$  the effective frequency  $\lambda_{eff}(z) = \mathcal{H}(z) - \beta(z)/[2P(z)]$ . In practice, both definitions from above are giving similar results, and we will mainly use (4).

In all our simulations we use a single-site excitation as the initial condition:  $\psi_l(0) = \delta_{l, l_c}$  with  $l_c = N/2$ , such that  $\lambda(0) = -\epsilon_{l_c}$  and  $P(0) = 1$ . In order to maximize the number of possible resonances with NMs, we have imposed that  $\epsilon_{l_c} = -W/2$ . With that and for  $c_0 > 0$ , the effective frequency will decrease starting from  $\lambda_{eff} = W/2$  until it reaches the bottom of the spectrum  $\lambda_{bot}$  where we stop our simulations. The bottom of the spectrum of an infinite system is located at  $\lambda = -2 - W/2$ . However, for finite systems the bottom of the spectrum  $\lambda_{bot} \geq -2 - W/2$  depends on the given realization. From (4) we see that a positive increment in  $\beta$  will decrease the effective frequency of the system. Therefore, the state will be able to resonate with other NMs inside the spectrum. Outside of it, the solution transforms into a self-trapped localized state similar to a discrete soliton [8,9,15], which is a time-periodic and exponentially localized excitation [3].

### III. NUMERICAL RESULTS

In Fig. 3 we show the evolution of an initial single-site excitation for  $W=3$  and  $N=100$ , when  $\xi < N$ . For  $c_0=0.2$ , a slow increase of nonlinearity leads to a complete delocalization of the wave packet at  $z \approx 800$ . Indeed, the effective frequency  $\lambda$  decreases and around that time reaches the bottom of the spectrum. At the same time, the participation number reaches its saturation value  $P \approx N/2 = 50$ . For a larger ramping velocity  $c_0=1$ , but exactly the same disorder realization, the wave packet does not spread over the entire chain. At a much shorter time  $z \approx 70$ , the effective frequency touches the bottom of the spectrum, the participation number saturates around  $P \approx 20$ , and the state becomes self-trapped, still occupying only 20 out of 100 sites.

Further increase of the ramping velocity will make the final wave packet more and more localized.

In order to study the dependence of the delocalization process on the disorder strength, we define our simulation scheme as follows: (i) we ramp the nonlinearity for a given velocity  $c_0$ ; (ii) we stop the simulation when  $\lambda_{eff}$  reaches the bottom of the spectrum  $\lambda_{bot}$ , indicating a stop of spreading due to self-trapping; (iii) we compute  $P$ , and if  $P < 40$ , we decrease the velocity  $c_0$  until  $P > 40$ , which corresponds to a fully delocalized wave packet. Therefore we obtain the critical velocity  $c_c$  for a given disorder realization. For  $c_0 > c_c$  the wave packet does not spread over the entire chain, while for  $c_0 < c_c$  it does. We repeat the scheme for 100 different disorder realizations and obtain an average value for  $c_c$ . Finally we change the disorder strength  $W$  and obtain the dependence  $c_c(W)$ . Results are shown in Fig. 4.

We observe two different regimes. For strong disorder  $W > 1$  the localization length is smaller than the system size  $N=100$ . The critical velocity  $c_c$  is monotonously decreasing

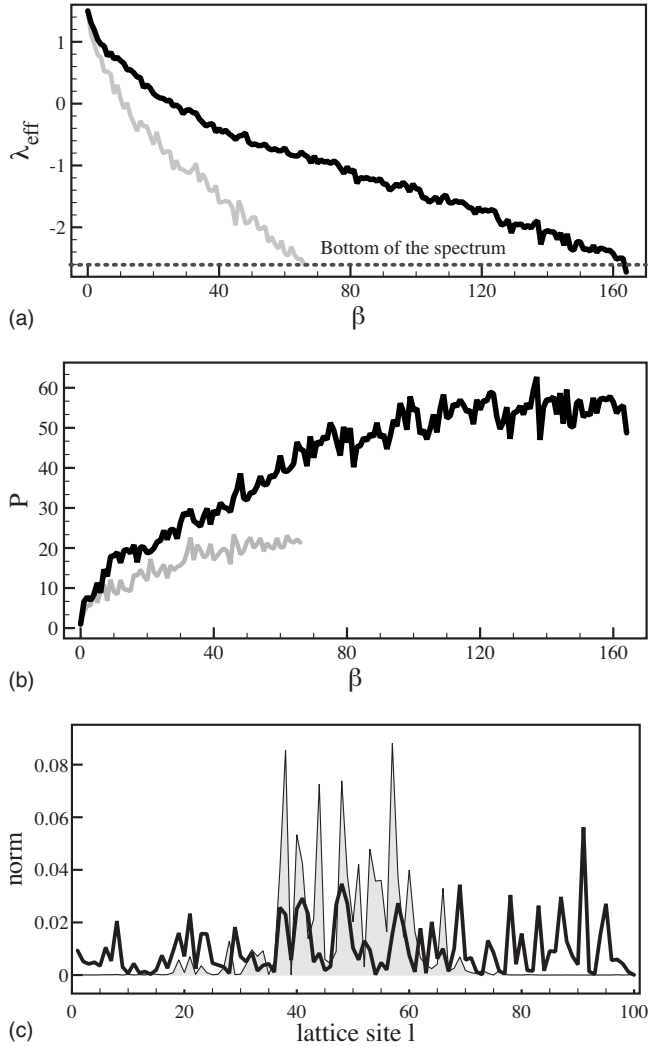


FIG. 3. Nonlinear propagation. (a)  $\lambda_{\text{eff}}$  versus  $\beta$ , (b)  $P$  versus  $\beta$ , and (c) final profiles. Gray and black curves correspond to  $c_0=1$  and 0.2, respectively.  $W=3$  and  $N=100$ . The horizontal dashed line in (a) corresponds to  $\lambda_{\text{bot}}$ .

with increasing disorder strength. This can be expected, since the stronger the disorder, the more localized the NMs are and the less is the number of other NMs a given NM can interact with due to nonlinearity. Therefore we need slower ramping in order to give ample time to NMs to interact. For weak disorder  $W < 1$  the localization length is larger than the system size  $N=100$ . Therefore all NMs are essentially extended over the entire chain. In this regime, we observe that the critical velocity  $c_c$  increases with increasing disorder strength. This effect may be due to the fact that in the limit of zero disorder  $W=0$ , the nonlinearity induces a selective interaction between NMs, as mentioned above (for details of that selective interaction, see Ref. [22]). Weak but nonzero disorder removes the selection rules and leads to an interaction of all modes with each other, thereby increasing the number of available modes (channels) by a factor of 2. The nonlinearity-induced spreading is more effective. In particular, it can redistribute the energy into 2 times more modes.

The hallmark of the transition from weak to strong disorder is the maximum in the dependence of  $c_c(W)$  at  $W=1$ . The

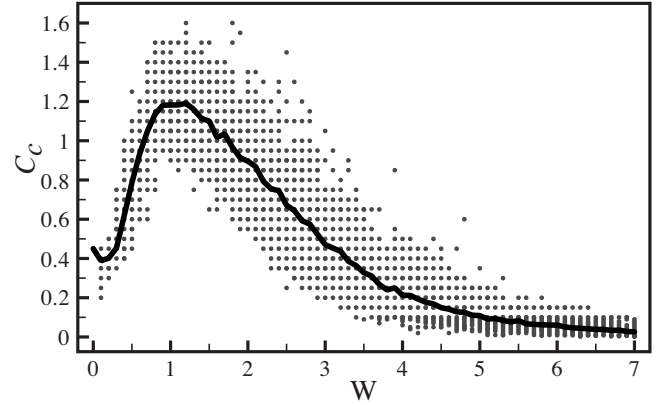


FIG. 4. Critical velocity versus degree of disorder for 100 realizations. The line represents the average  $c_c$ .  $N=100$ .

maximum is located at  $W \sim \sqrt{100/N}$ . In particular, for  $N=50$  it is located at  $W \sim 1.4$  and for  $N=200$  at  $W \sim 0.7$ . For large  $N \gg \xi$  the maximum position is therefore shifted closer to  $W=0$ , and the value in the maximum increases. The value of  $c_c$  at  $W=0$  can be estimated by noting that the fastest plane waves reach the edges of the chain at a time  $z_b \approx N/4$ . The time it takes to shift the frequency of the initially excited oscillator out of the band is  $z_s \sim 4/c_0$ . Equating  $z_b = z_s$  we estimate  $c_c(W=0) \sim 16/N$ . The increase of this critical speed in the presence of weak disorder is due to the above-discussed increase of modes (channels) available. This increase by a factor of 2 leads to a decrease of the norm in each mode also by a factor of 2, consequently implying a larger critical velocity. Therefore  $z_s \sim 2/c_0$  and  $\max[c_c(W \neq 0)] \sim 2c_c(W=0)$  at best. This increase by a factor of 2 is close to the numerical observation (see Fig. 4).

#### IV. DISCUSSION: DIFFUSION VERSUS RESONANT SPREADING

Let us discuss possible mechanisms of wave packet spreading in the regime of strong disorder, when  $\xi < N$ . The packet spreading beyond the localization volume is entirely due to the nonlinearity, which induces interactions between NMs. Assume the wave packet has a certain size at some time  $z$ . Further spreading implies excitation of exterior NMs. Since the interaction between NMs falls off exponentially for distances larger than  $\xi$ , the relevant exterior NMs to be excited will be located in a nonexcited (cold) boundary layer outside the wave packet, with a width roughly of the order of the localization volume. A given cold exterior NM can be excited coherently or incoherently. A coherent excitation implies a resonance with an excited NM from the wave packet and a corresponding resonant transfer of energy (as happens during the beating of energy between two weakly coupled harmonic oscillators). An incoherent excitation implies an almost random fluctuation of the NMs phases inside the wave packet. It generates a random force which incoherently excites (heats) the exterior NMs. It finally results in a diffusive spreading of the wave packet, therefore of the norm, and the energy.

### A. Diffusion

The spreading of wave packets in the presence of a constant nonzero nonlinearity strength  $\beta = \beta_0$  was studied in several papers [11–14]. In particular, it was observed, that a spreading wave packet is characterized by a growth of its second moment  $m_2 \sim z^\alpha$ . The exponent  $\alpha = 0.33 \pm 0.02$  [13]. A theoretical analysis suggested that this subdiffusive spreading is not due to resonant excitation of exterior modes, but due to incoherent heating, which is caused by a chaotic dynamics of the NMs inside the core of the packet. The origin of the chaotic dynamics of the wave packet itself comes from a resonant interaction of NM pairs inside the packet [13]. The statistical analysis of the probabilities of such internal resonances leads to the conclusion that the second moment obeys the following equation:

$$\frac{dm_2}{dz} = C(W)\beta^4 n^4. \quad (5)$$

Here  $n$  is the average norm density inside the wave packet and  $C(W)$  an unknown function, which, however, as numerical studies suggest, decreases with increasing  $W$ . Since the packet size is  $\sim 1/n$ , it follows that the participation number  $P \sim 1/n$  and the second moment  $m_2 \sim 1/n^2$ . As a consequence,  $m_2 \sim (\beta^4 z)^{1/3}$  [13]. The exponent  $\alpha = 1/3$  is in very good agreement with the numerical studies. The nonlinearity-induced frequency shift inside the packet  $\delta\lambda \sim \beta n \sim z^{-1/6}$ . The more the packet spreads, the smaller the frequency shifts are. This weakening is counterbalanced by an increase in the size of the packet. The larger that size, the more modes are involved, and the probability of finding a resonant pair interaction increases. These two effects—weakening of the nonlinear frequency shifts, on the one hand, and the increase of the number of involved modes, on the other hand—are predicted to counterbalance each other, so that on average a finite number of packet modes is interacting resonantly. These resonances lead to weak chaos and decoherence of phases of NMs, and thereby guarantee a slow but steady subdiffusive spreading [13].

Assuming that in the present case the spreading is incoherent as well, we find with  $\beta = c_0 z^\mu$  and (5)

$$m_2 \sim c_0^{4/3} z^{(4\mu+1)/3}, \quad P \sim c_0^{2/3} z^{(4\mu+1)/6}. \quad (6)$$

The nonlinearity-induced frequency shift

$$\delta\lambda \sim \beta n \sim z^{(2\mu-1)/6}. \quad (7)$$

In the present numerical studies  $\mu = 1$ , and we find  $m_2 \sim z^{5/3}$ ,  $P \sim z^{5/6}$ , and  $\delta\lambda \sim z^{1/6}$ . At variance with the case of constant nonlinearity (which yields subdiffusion with  $\alpha = 1/3$ ), we obtain superdiffusion with  $\alpha = 5/3$ . This is due to the fact that the increasing nonlinearity counterbalances the decay of the frequency shifts and enhances the interaction of the NMs from the wave packet with cold exterior NMs. The growth of the frequency shifts will finally lead to a self-trapped state, as observed in numerical studies.

Let us estimate the dependence of the participation number  $P$  of the self-trapped wave packet on  $c_0$ . With Eq. (6) it follows that

$$n \sim c_0^{-2/3} z^{-(4\mu+1)/6}. \quad (8)$$

Therefore the nonlinear frequency shift  $\delta\lambda = \beta n \sim c_0^{1/3} z^{(2\mu-1)/6}$ . When this frequency shift reaches some finite (disorder dependent) value at  $z = z_f$ , the wave packet self-traps. Therefore  $z_f \sim c_0^{-2/(2\mu-1)}$ . Finally

$$P(z_f) \sim \frac{1}{n(z_f)} \sim c_0^{-1/(2\mu-1)}. \quad (9)$$

For  $\mu = 1$  we find that the self-trapped wave packet has size  $P \sim 1/c_0$ . Increasing the ramping speed  $c_0$  therefore leads to a smaller extent of the self-trapped wave packet, as observed in numerical results. We cannot estimate the measured dependence  $\bar{c}_c(W)$ , since we do not know the function  $C(W)$  from (5).

### B. Resonant spreading

Let us assume that the wave packet spreads by resonantly exciting exterior NMs. Except for exponentially small ramping velocities, the relevant exterior NMs will be located in a layer of the width of the localization volume. The average frequency spacing  $\Delta\lambda \approx \Delta/\bar{p}$  separates possible frequencies of resonant interactions, which can take place due to the nonlinearity-induced frequency shift. Therefore the number of possible resonances is limited to the number of NMs within one localization volume—i.e. to the localization volume  $\bar{p}$  itself. Let us assume that each resonance leads to a population of a mode at the maximum distance  $\bar{p}$ . After that, two modes are excited, with a some distribution of norm among them and therefore smaller nonlinearity-induced frequency shifts. Assume that this process continues. It will stop when the nonlinearity-induced frequency shift is less than the average frequency spacing. Therefore, we can excite of the order of  $\bar{p}$  NMs, each at a distance of  $\bar{p}$  from the next one. The maximum size to which a wave packet can grow is then proportional to the  $\bar{p}^2$ . The numerical results in Fig. 4 show that for strong disorder  $W = 7$  the critical velocities are of the order of  $c_c \approx 0.01$ . For such a velocity the wave packet spreads completely over a chain with 100 sites. The maximum localization length  $\xi \approx 2$ ; therefore, the localization volume is less than  $\bar{p} \approx 7$  and the maximum size is less than  $\bar{p}^2 \approx 50$ , which indicates that resonant spreading is not the dominant mechanism.

Let us assume the optimum case scenario for resonant spreading. That implies that at a given time a resonance at the edge of the wave packet can take place and the energy is transferred much faster than it takes to shift the frequency to the next resonance. Assume we start with one NM excited, with its frequency located at the edge of the spectrum. For  $\mu = 1$ , we will hit the next possible resonance after time  $z_1 = \Delta\lambda/c_0$ . We assume that a resonant mode is available in the localization volume and is immediately excited. The norm is now equally distributed between both NMs, each of them having norm  $1/2$ . Nonlinearity is further ramped up, but in order to shift the frequency to the next resonance, a larger time  $z_2 = 2z_1$  is needed, and so on. As long as the wave packet does not self-trap, we find  $z_j = jz_1$ . Therefore the total time to reach the  $j$ th resonance scales as  $z \sim j^2$ , the participation

number  $P \sim j$  grows as  $P \sim \sqrt{z}$ , and the second moment  $m_2 \sim z$ . Since that idealized process is already slower than the incoherent spreading due to diffusion, we expect that resonant spreading is weakly contributing to the numerically observed spreading.

## V. CONCLUSIONS

We have investigated how to control the spreading of a wave packet in a disordered nonlinear chain when ramping the nonlinearity in time. We studied the case of a finite chain and computed the critical ramping speed  $c_c$ , which separates self-trapped localized from self-trapped delocalized states at the end of the ramping process. We find that  $c_c$  grows with increasing strength of disorder when the localization length is larger than the system size. This increase is due to the fact that disorder is removing selection rules for the interaction of normal modes, present in the case of zero disorder. For strong disorder—i.e., when the localization length becomes smaller than the system size—the critical velocity drops with further increase of the disorder strength, which is due to the fact that the normal modes are less and less spread, interact

with fewer other modes, and the nonlinearity-induced frequency shift is more efficient in tuning the wave packet faster into a self-trapped state. For linear ramping  $\mu=1$ , we find that the spreading is mostly due to incoherent diffusive processes. For an infinite chain, the nonlinear frequency shift always leads to a self-trapping of the wave packet, and therefore not to a complete delocalization. The second moment  $m_2 \sim z^{5/3}$  is predicted to grow superdiffusively, at variance with the previously studied case of constant nonzero nonlinearity [13], which yields subdiffusion. Therefore the present case is easier accessible in finite system's experiments, due to possible restrictions on maximum propagation times. Controlling the localization and delocalization properties of a spatial state, in a finite lattice, could open many possibilities for technological applications in optics as well as in cold atoms physics.

## ACKNOWLEDGMENTS

We thank B. Altshuler, S. Komineas, D. Krimer, and Ch. Skokos for useful discussions. R.A.V. acknowledges financial support from FONDECYT (Grant No. 1070897).

- 
- [1] O. Morsch and M. Oberthaler, *Rev. Mod. Phys.* **78**, 179 (2006).
- [2] F. Lederer, G. I. Stegeman, D. N. Christodoulides, G. Assanto, M. Segev, and Y. Silberberg, *Phys. Rep.* **463**, 1 (2008).
- [3] S. Flach and C. R. Willis, *Phys. Rep.* **295**, 181 (1998); D. K. Campbell, S. Flach, and Yu. S. Kivshar, *Phys. Today* **57** (1), 43 (2004); S. Flach and A. V. Gorbach, *Phys. Rep.* **467**, 1 (2008).
- [4] P. W. Anderson, *Phys. Rev.* **109**, 1492 (1958).
- [5] L. Guidoni, C. Triché, P. Verkerk, and G. Grynberg, *Phys. Rev. Lett.* **79**, 3363 (1997).
- [6] B. Damski, J. Zakrzewski, L. Santos, P. Zoller, and M. Lewenstein, *Phys. Rev. Lett.* **91**, 080403 (2003).
- [7] J. Billy *et al.*, *Nature (London)* **453**, 891 (2008); G. Roati *et al.*, *ibid.* **453**, 895 (2008).
- [8] T. Pertsch, U. Peschel, J. Kobelke, K. Schuster, H. Bartelt, S. Nolte, A. Tünnermann, and F. Lederer, *Phys. Rev. Lett.* **93**, 053901 (2004).
- [9] Y. Lahini, A. Avidan, F. Pozzi, M. Sorel, R. Morandotti, D. N. Christodoulides, and Y. Silberberg, *Phys. Rev. Lett.* **100**, 013906 (2008).
- [10] T. Schwartz, G. Bartal, S. Fishman, and M. Segev, *Nature (London)* **446**, 52 (2007).
- [11] D. L. Shepelyansky, *Phys. Rev. Lett.* **70**, 1787 (1993); M. I. Molina, *Phys. Rev. B* **58**, 12547 (1998).
- [12] A. S. Pikovsky and D. L. Shepelyansky, *Phys. Rev. Lett.* **100**, 094101 (2008); I. Garcia-Mata and D. L. Shepelyansky, e-print arXiv:0805.0539v1.
- [13] S. Flach, D. O. Krimer, and Ch. Skokos, *Phys. Rev. Lett.* **102**, 024101 (2009).
- [14] G. Kopidakis, S. Komineas, S. Flach, and S. Aubry, *Phys. Rev. Lett.* **100**, 084103 (2008).
- [15] G. Kopidakis and S. Aubry, *Phys. Rev. Lett.* **84**, 3236 (2000); *Physica D* **130**, 155 (1999); **139**, 247 (2000).
- [16] T. Schulte, S. Drenkelforth, J. Kruse, W. Ertmer, J. Arlt, K. Sacha, J. Zakrzewski, and M. Lewenstein, *Phys. Rev. Lett.* **95**, 170411 (2005).
- [17] L. Khaykovich, F. Schreck, G. Ferrari, T. Bourdel, J. Cubizolles, L. D. Carr, Y. Castin, and C. Salomon, *Science* **296**, 1290 (2002).
- [18] A. Szameit, J. Burghoff, T. Pertsch, S. Nolte, A. Tünnermann, and F. Lederer, *Opt. Express* **13**, 10552 (2005).
- [19] D. Kip (private communication).
- [20] B. Kramer and A. MacKinnon, *Rep. Prog. Phys.* **56**, 1469 (1993).
- [21] A. D. Mirlin, *Phys. Rep.* **326**, 259 (2000).
- [22] K. G. Mishagin, S. Flach, O. I. Kanakov, and M. V. Ivanchenko, *New J. Phys.* **10**, 073034 (2008).